Geotechnical Testing Journal, Vol. 29, No. 6
Paper ID GTJ100304
Available online at: www.astm.org

Zhibin Liu,[1] *Bin Shi,*[2] *and Daichao Sheng*[3]

A Micropenetrometer for Detecting Structural Strength Inside Soft Soils

ABSTRACT: A micropenetrometer is developed to measure structural strength inside soft soils. Different from the traditional detective technology for soil structure, the micropenetrometer is an intrusion technology to estimate the characteristics of soft soils. The work principle and main configuration of the micropenetrometer are introduced, followed by its calibration and some operation techniques. Finally, two application tests are carried out. Different soil textures such as sandy soil or clayey soil have different types of penetration curves. Through the end resistance variation, detailed description of the structural strength along penetration depth can be obtained. In addition, three-dimensional strength distribution on the vertical or transverse sections can be achieved from the penetration data evenly arranged on the grid nodes of the same surface through interpolation method. Such a technique is of significance for checking the effectiveness of soil improvement or monitoring the moisture movement in soil.

KEYWORDS: structural strength, soft soil, penetration resistance, micropenetrometer

Introduction

In geotechnical practice, soils are usually treated as homogeneous or ideal anisotropic materials. However, real soil behavior is rather nonlinear, discontinuous, heterogeneous, anisotropic, and uncertain, and sometimes these properties and their evaluation become quite important. To understand the internal structural mechanism of soils, many kinds of apparatuses have been developed such as the optical microscope (Smart and Tovey 1966), mercury intrusion porosimeter (Prapaharan et al. 1985; Lapierre et al. 1990), scanning electron microscope (Tovey and Krinsley 1992; Shi and Li 1995; Katti and Shanmugasundaram 2001), and computerized tomography (Otani et al. 1997; Li and Zhang 1999; Tamotsu et al. 2001). Some apparatuses normally used in other fields are also introduced into soil microstructural research, such as electrical resistivity (Fukue et al. 1999), automatic adsorption apparatus (Liu et al. 2004), and so on. These traditional microstructural research tools are used mainly for the study of soil fabric, such as texture, aggregate arrangement, void size and distribution, etc. The key limitation of these apparatus is that they cannot analyze or characterize the structural strength distribution inside soils, which in fact reflects the bonding energy between soil aggregates or units. For the convenience of research, the structural strength can be defined here as the referenced magnitude of intrusion force with a certain probe to break apart or pass through a microstructural unit of a soil. However, it is sometimes significant to know the strength distribution inside a soil and the trend of their variations. For example, in soil modification tests, engineers care about how uniformly the additive has been mixed if the objective is to improve the macroscopic strength of the soil. In the relatively new modeling technology of soil behavior, the soils need to be modeled both macroscopically and microscopically. Therefore, knowledge on the microscopic strength variation of a soil is of significance. It is also known that the moisture content has a great influence on the mechanical properties of soils. Moisture infiltration and movement inside a soil can change its microstructure especially its local structural strength intensively. Therefore, through research work on the variation of structural strength inside a soil, we can know the distribution and variation of moisture inside it from a different perspective. To the authors' knowledge, there are few specific apparatuses with which the structural strength distribution inside soils can be measured quantitatively. Though various cone penetrometers have been extensively adopted in soil science and engineering practice to identify soil profiles (Henderson 1989) or to predict soil properties (Ayers and Bowen 1987), these tests usually reflect the strength of a large soil body only, and cannot do much on the microstructural scope.

From the discussion above, it is easy to think that a more reasonable and effective way to detect the structural strength of a soil is to use a special penetrometer of quite small dimension. Research experience shows that the measured penetration resistance of a traditional penetrometer depends on soil properties such as bulk density, water content, aggregation, cementation, and mineralogy. Furthermore, the measurements are also affected by operational parameters, such as cone shape, size, construction material, and penetration speed (Gill 1968; Whiteley and Dexter 1981). However, if the statistical structural strength distribution of a soil under certain circumstances has been found, it is possible to establish the relationships between the microscopic physical properties of a soil and its structural strength, and even the macroscopic mechanical properties. A quite similar idea has been successfully implemented in the research work of snow strength to explore those thin and weak layers for the prediction of avalanche (Schneebeli and Johnson 1998).

As an attempt to detect and analyze the structural strength of soft soils in engineering, a specific micropenetrometer has been developed and introduced in this paper, which may lead to various possibilities for research work related to soft soils. Finally, two simple application experiments are also described to prove its workability and feasibility.

Manuscript received May 20, 2005; accepted for publication May 19, 2006; published online July 2006.

[1]Research Staff, Discipline of Civil, Surveying and Environmental Engineering, The University of Newcastle, NSW, Australia, 2308.

[2]Professor, ACEI, Department of Earth Sciences, Nanjing University, Nanjing, China, 210093.

[3]Associate Professor, Discipline of Civil, Surveying and Environmental Engineering, The University of Newcastle, NSW, Australia, 2308.

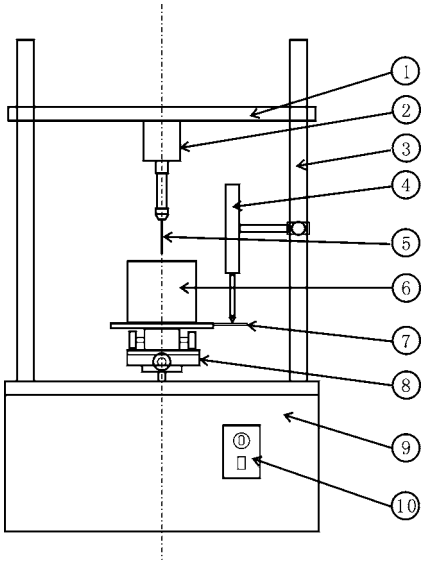

FIG. 1—*Buildup of the micropenetrometer. 1. Crossbeam. 2. Load cell. 3. Vertical shaft. 4. Displacement transducer. 5. Penetration probe. 6. Container. 7. Loading disk. 8. Traverse stage. 9. Control box. 10. Control panel.*

Configuration and Operation of the Micropenetrometer

Mechanical Analysis

When a rigid cylindrical probe penetrates into a soil vertically at a uniform and low speed, the higher the structural strength the soil, the greater the resistance to the penetration will be, and vice versa. During the course of penetration, resistance which the probe bears includes the end resistance and the peripheral friction. While, when the probe withdraws from the soil at the same speed, it only endures the peripheral friction. If a load cell is installed at the opposite end of the probe, the total resistance during penetration and the friction during withdrawal can be easily measured. Through some data process, the peripheral friction at any penetration depth can be deducted from the total resistance. The dependence of the end resistance and the corresponding penetration depth can thus be obtained. Accordingly, the end resistance of the probe at a certain penetration depth can be taken as a reference value of the structural strength of the soil at this position. Thus, it is obvious that if the probe is rigid and slim enough the structural strength distribution of a soil can be achieved through a series of penetration tests.

Based on the work principle discussed above, a SMP-1 micropenetrometer was designed by the Advanced Computational Engineering Institute for Earth Environment of Nanjing University.

Configuration

The SMP-1 micropenetrometer is basically made up of two systems: mechanical control and positioning system, data collection, transfer and storage system.

The buildup of the micropenetrometer is shown in Fig. 1. The main framework of the mechanical part constitutes two vertical shafts and the bottom control box. A crossbeam is connected to the shafts through two bolts being able to adjust the position of the crossbeam so that the sample container can be installed easily. For the measurement of the penetration resistance, a probe is, through a special holder, connected to a sensitive load cell that is fixed on the crossbeam. Soil sample is put inside the container, which is seated on a loading disk. Having the same size diameter with a typical mold for compaction test, the cylindrical container can also be split into two semi-cylindrical parts so that even the normal remolded soil sample can be easily installed in it. In the design of this micropenetrometer, there is one thing different from the traditional penetration techniques: it is the sample, not the probe, that moves to decide the penetration points on soil surface. Here, a traverse stage is adopted as a positioning mechanical part since the loading disk is just installed on it. With two layers of perpendicular dovetail grooves on the stage the soil container can glide in two orthogonal directions by just turning the control knobs. The scale on dovetail grooves is the same with that of a vernier caliper, so it ensures that the resolution of the displacement adjustment would reach 0.5 mm. Inside the bottom control box there is a constant speed electrical rotary motor, which is the key component of a stepless speed change device. This device can push the whole traverse stage upward and pull it back at a uniform speed through a worm gear drive system. Fixed to the shafts, the probe is kept motionless during a test, but the soil can move toward and away from it relatively. Thus, when the micropenetrometer works, the process of penetration and withdrawal can be realized easily through the mechanical control and positioning system.

The data collection, transfer, and storage system contain mainly the load cell, the displacement transducer, data wires, a condition catcher, a computer, and a set of control software. The load cell can measure any resistance of compression or tensile force. While, with a range of 50 mm and a resolution of 0.1 mm the displacement transducer attached to the right-handed shaft can capture the distance the soil container has passed when it moves upward and downward. Resistance forces and penetration depths measured by the two transducers will be input into a condition catcher, and are then sent to a computer for post-treatment. The condition catcher is actually a multifunctional data logging system that can collect and store the analog signals or even digital signals temporarily. As a powerful tool for the data collection, it has eight input channels for the same number of sensors at a time. During the course of measurement, the analogtodigital conversion signals acquired can be transferred to the hard disk at quite a high speed through USB communication between the condition catcher and the computer. Finally, through the software data, values can be displayed on screen or stored in a data file. Specially equipped for the control of condition catcher and illustration and management of the final data, the sampling method and period in measurement, illustration style, and file format for the final data can be selected.

Because different soils, even the same soil with different water content, can have distinct structural strengths, the micropenetrometer is equipped with a series of penetration probes with various diameters from 0.3 to 1 mm, which can be selected according to the research objective and soil properties. Each probe has a certain peripheral influence area because of the squeezing effect when it penetrates into a soil sample. Researchers should first judge whether or not the probe diameter will affect the resolution distance of their research zone. On the other hand, since the probe is not an ideally rigid body, no matter how hard the probe material is, it will bend especially when the structural strength of the soil is relatively hard for some special kinds of soil or soils with low moisture content, which will hurt the reliability of the test data. Thus, the probe diameter should be great enough to eliminate the bending effect under the condition that it can meet the resolution distance requirement. Since the capacity of load cell is 100 N and its resolution is 0.1 N,

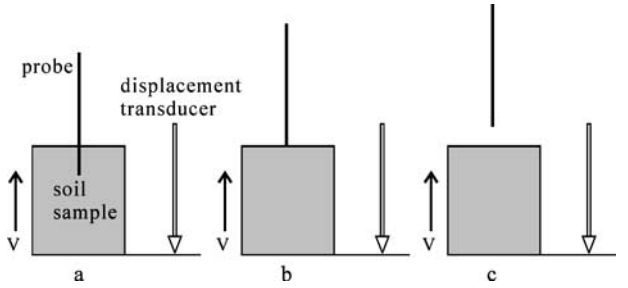

FIG. 2—*Possible relative states for the probe and displacement transducer.*

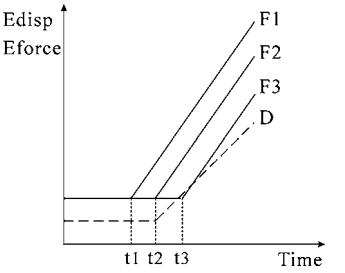

FIG. 3—*Response curves of the load cell and displacement transducer at the beginning of the penetration.*

the structural strength of soil sample should not be too high. Therefore, suitable test samples for this apparatus should be soft soils.

The relative penetration velocity of the probe can be adjusted to a constant value between 1 and 5 mm/min so as to get a reference standard rate. All parallel tests should adopt a same penetration speed since different structural strength values may be achieved under different penetration speed though the difference is generally not large. Through many practical experiments, it is found that the penetration velocity of the probe should not be too great. If the velocity is too high, it may add unnecessary extra destroy to the soil sample. For example, when the probe runs from a hard layer into a soft layer there may be a sudden impact because of the energy release, which must be avoided during the overall experiment. A reasonable velocity should be very slow and uniform all the time.

Calibration

Measurement data collected from the load cell and displacement transducer are voltage signals. Further calibration work must be made to achieve the calibration coefficients so that the final data can be transformed into the real value of resistance force [N] and displacement [mm]. After many repeated tests the following two calibration linear equations are obtained. They represent the transformation relationship between the measured voltage signals (*Edisp* and *Eforce*) and the real values (*PeneDisp* and *Peneforce*):

$$PeneDisp = (Edisp)10 + 0 \text{ [mm]} \tag{1}$$

$$PeneForce = (Eforce)20.05 - 1.75 \text{ [N]} \tag{2}$$

The calibration coefficients and the constant in above equations may change as the mechanical life of the micropenetrometer, so that calibration coefficients should be corrected frequently.

Techniques for Operation

The diameter of the probe in the micropenetrometer is so small that the displacement transducer has to be installed separately from it, which results in the difficulty of penetration depth capture. If the initial position of the soil container is neglected carelessly, usually it cannot be ascertained that when the probe contacts the soil surface, the displacement transducer begins to measure the penetration depth simultaneously. However, through some techniques we can resolve this problem reasonably.

There are overall three possible relative states for the probe and displacement transducer which corresponds to *a*, *b*, and *c* in Fig. 2. In state *a*, after the probe penetrates into the soil sample the displacement transducer begins to work, and the response curves of the penetration resistance and the displacement are F1 and D in Fig. 3. In state *b*, as the probe contacts the soil surface the transducer begins to work at the same time, and the response curves are F2 and D in Fig. 3. In state *c*, after the transducer has worked for a short period of time the probe begins to pierce into the soil, and the response curves are F3 and D in Fig. 3. Because the displacement transducer can detect any relative displacement after time t2, the exact penetration depth can be achieved in state *b* and *c*. Thus, during an experiment a reliable technique is to make the displacement transducer work earlier than the penetration of the probe through some simple state adjustment as Fig. 2.

Another important thing should be noticed is that reasonable selection of penetration points can save much trouble for the future structural strength analysis. Since the traverse stage can only move in two orthogonal directions, here imaginary equidistant lattice arrangement on the surface of the sample is recommended, and the mutual origin of the scales on two dovetail grooves is set as the origin of *x* and *y* on horizontal surface. During experiment, we first adjust the probe to the exact position right above each grid node, and record the corresponding coordinates. We then start up the control software on the computer to set the sampling conditions, turn on the motor, and let the probe pierce into the sample. When the probe reaches its scheduled depth, we stop the motor temporarily, and then switch it to the inverse direction. After the probe has withdrawn from the soil, we store the data for later post-treatment and turn off the micropenetrometer.

Figure 4 is a schematic diagram of penetration lattice arrangement. During the data post-treatment, from one penetration point (in other words, penetration data along a penetration axial line) if the friction at each depth is deducted from corresponding total penetration resistance, the relationship curve of end resistance and penetration depth will be achieved. If all test points on a plane with same *x* value are combined, an isogram of the structural strength distribution on a vertical section of the sample can be obtained, which is also adequate for a vertical section with same *y* value.

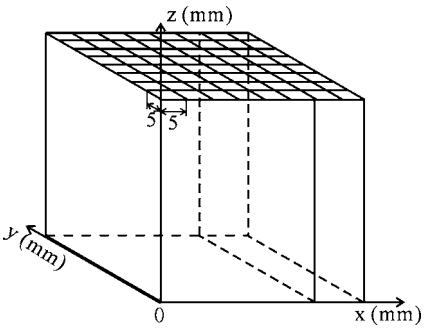

FIG. 4—*Schematic diagram of penetration lattice arrangement.*

TABLE 1—*Physical properties of the tested sandy soil.*

					Grain Size Distribution			
Natural Water Content, %	Natural Density, g/cm^3	Void Ratio	Average Diameter, mm	Coefficient of Nonuniformity	<0.05, mm	0.07–0.05, mm	0.25–0.075, mm	>0.25, mm
37	1.7	0.68	0.2	2.7	9	37.5	51.5	2

Similarly, if all test points on a plane of same depth (z value) are organized, a strength contour map on a transverse section will also be extracted. Furthermore, if all these isograms are put into analysis together, a three-dimensional structural strength distribution inside the sample will finally be known.

Application Tests

As part of verification work for its feasibility, several application tests of the micropenetrometer are introduced here. For the convenience of analysis and explanation, the penetration velocity is controlled at 5 mm/min in the later application tests with a probe of 1 mm in diameter. The lattice space adopted here is 5 mm (Fig. 4), and the sampling period is set to 0.01 s.

Penetration Curves of Different Materials

It can be speculated that soils of different texture may have different typical structural strength. As an example, three kinds of soil are tested by the micropenetrometer. The first one is an undisturbed sample of sandy silt which is collected from a light rail construction site of Suzhou city. The physical properties of the sandy soil are given in Table 1. The second one is a remolded sample of a clayey soil which is widely distributed around Nanjing city, and it is compacted wet of its optimum moisture content. The last one is a cup of manually prepared sullage which is made from above clayey soil, and has cured over 12 h. Typical physical and mechanical properties of the tested clayey soil are listed in Table 2. Relation curves of different resistance and penetration depth are illustrated from Figs. 5–7. Friction curve is plotted according to the value measured when the probe withdraws from soil. End resistance is equal to the difference of the absolute values of total resistance and its corresponding friction during penetration.

It can be seen that for each sample when the probe breaks through soil surface the total and end resistance curves will increase sharply, which reflects the course of elastic deformation and adjustment of the system of probe and load cell to bear the structural strength of the surface layer in soil. However, it is actually much more complicated to clearly explain this short process be-

TABLE 2—*Physical and mechanical properties of the tested clayey soil.*

					inth			Grain Size Distribution		
Natural Water Content, %	Natural Density, g/cm^3	Degree of Saturation, %	Void Ratio	Liquid Limit, %	Plastic Limit, %	Cohesion, MPa	Angle of Internal Friction, deg	<0.005, mm	0.005–0.05, mm	>0.05, mm
15.9	1.96	64.0	0.677	32.4	18.7	90	29	28.24	64.76	7.0

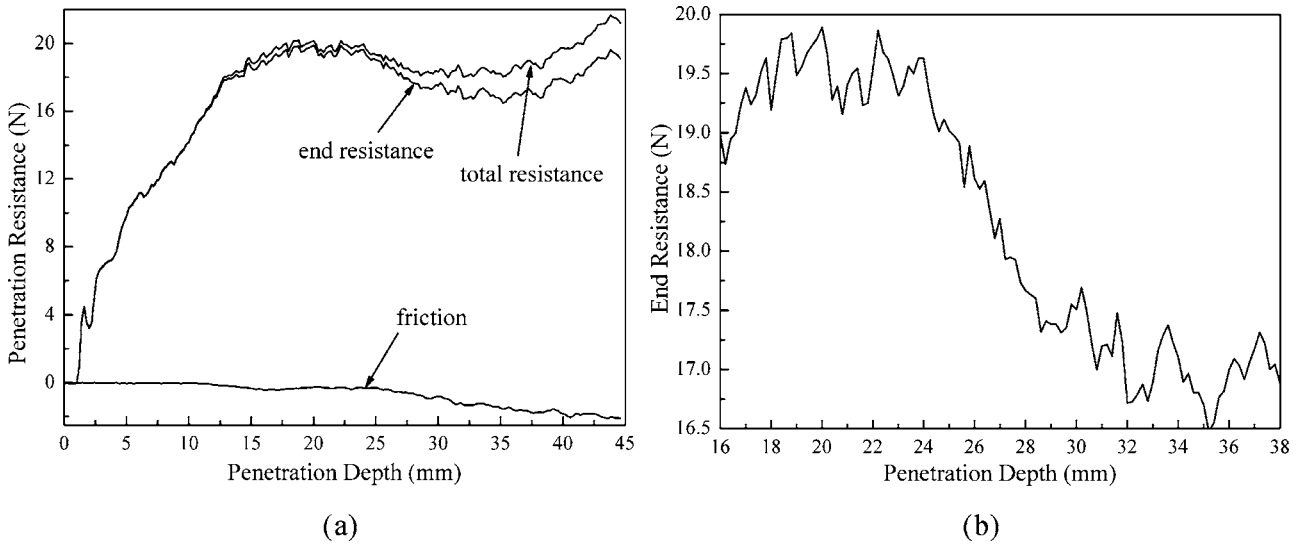

FIG. 5—*Penetration resistance curves of the sandy soil:* (*a*) *global curves;* (*b*) *ordinate enlarged detail of the end resistance.*

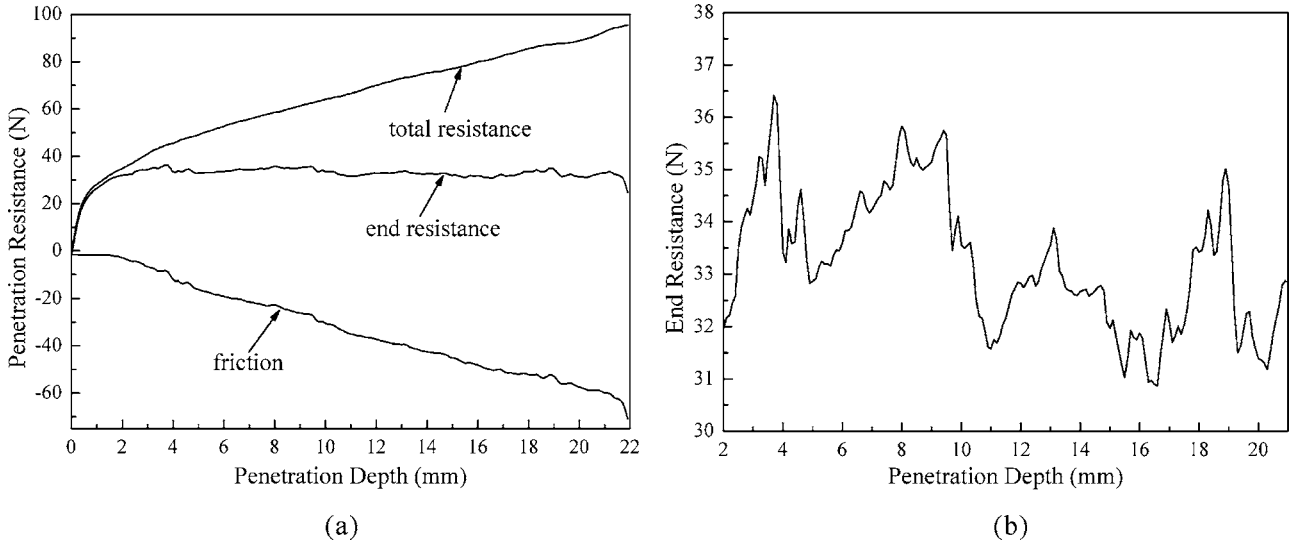

FIG. 6—*Penetration resistance curves of the remolded soil:* (*a*) *global curves;* (*b*) *ordinate enlarged detail of the end resistance curve.*

cause it also accompanies obviously synchronous deformation of soil surface including aggregate deflection, slippage, cleavage, and subsidence displacement. Sometimes, this kind of surface effect especially the subsidence displacement can have remarkable influence on the initial penetration stage. In some soil, if there is a slight clearance between its surface and inner part, such kind of subsidence during penetration will lead to obvious lag in the increase of end resistance. After continually climbing up at the beginning, the curve of end resistance enters into a horizontally developed stage, during which the penetration curve fluctuates according to the structural strength of soil. For friction along the penetration depth it is nearly linearly distributed but with some variance such as detailed fluctuations somewhere. Since the frictional coefficient may remain invariable for the same texture, fluctuations in the friction measurement can also reflect the structural strength in a sense because of the lateral stress exerted on the side of probe.

Sandy Soil from Suzhou Light Rail Construction Site

For sandy soil since there is little bonding force or cohesion between coarse-grained particles, structural strength here is mainly a representative of a regional compactness of soil mass. When the probe penetrates into sandy soil, the tip will touch and push sand particles downwards. Due to their high hardness, the sand particles are not easy to destroy and split by the probe, and they will try to compact those particles under them and gradually deflect and thrust away laterally so as to make room for the probe to move forward. It takes about 14-mm depth for the probe to reach a final steady penetration state, which may be explained by the compression of surface layer. The top layer of this sandy soil is constituted of porous sands coarser than that of the middle and bottom part. The low friction in this surface layer also indicates that sandy soil in this layer is relatively loose. Such a compaction procedure then reaches a limit, so that there is insignificant additional compaction effect contained in the penetration. Therefore, the following end resistance variation mainly comes from the reactive force for sand particles to deflect and thrust away. The higher the structural strength of the sandy soil the greater end resistance the probe will meet. It can be judged from the large curve valley of the end resistance in Fig. 5(*a*) that there exists a relatively soft interlayer between 30 and 40 mm in depth.

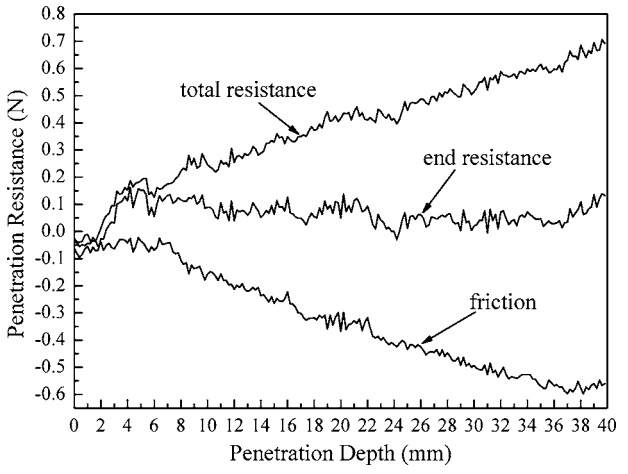

FIG. 7—*Penetration resistance curves of the sullage.*

However, a great advantage of the micropenetrometer puts emphasis on the measurement of microscopic structural strength variation in soil. A typical amplificatory end resistance curve of the sandy soil is shown in Fig. 5(*b*), from which it can be seen that in a same layer with similar average structural strengths, the end resistance variation has a quite similar waveform. Furthermore, most of these waves are single-peaked with quite approximate wavelength and wave height due to the special constituents of relatively homogeneous hard sand particles. Normally it needs 0.5 to 1.5 N for the probe to pass through each soil unit of high structural strength.

Remolded Clayey Soil

The clayey soil used in this test is a kind of soil widely distributed in Nanjing, a city in Eastern China. Natural undisturbed clayey soil has complicated inner structure, which makes its macroscopic soil strength often greater than that of remolded. As a simple application test for the micropenetrometer, a remolded sample is made for experiment through standard laboratory test. Because of the destruction of its original microstructure the remolded clayey soil becomes much homogeneous and isotropic than before, which can be

proved by the nearly horizontally developed end resistance curves for various penetration point and different penetration orientation in the sample without many large peaks or valleys (Fig. 6(*a*)).

During the period of steady penetration, average end resistance is between 30 and 40 N for the remolded clayey soil. It only takes the probe not more than 2 mm to reach its final steady penetration state, as indicates that obvious surface compaction effect does not exist in clayey soil. This can be explained by the totally different constituent and texture of clayey soil compared with sandy soil. Mainly consisted of fine grained particles smaller than 0.06 mm, clayey soil is usually plastic and cohesive under certain moisture content. Hard primary minerals and clay minerals first form small aggregates, then combine into relatively soft large aggregates, and finally join together as clayey mass. It is found that small aggregates often have greater structural strength than large ones (Braunack et al. 1979; Hadas 1987). Large inter-aggregate pores construct great weak zones, while tiny intra-aggregate voids formulate small soft spots. Due to special properties of clayey soil, a probe of the micropenetrometer can pierce into and split clay aggregates easily without their remarkable deflection, rotation and lateral displacement. An ordinate enlarged detail of the end resistance curve for the clayey soil is shown in Fig. 6(*b*), from which the average end resistance evaluated is about 33 N for the overall penetration course. However, detailed resistance variation in Fig. 6(*b*) indicates that different parts of the remolded soil can have inequable structural strength. Unlike the sandy soil, the end resistance curve of clayey soil is not just consisted of a series of similar small waves. It is formed by many large waves that further contain some small ones. Large waves actually represent the global end resistance evolution when the probe penetrates through big soil aggregates, and small waves stand for the structural strength variation inside. It normally takes about 3 to 6 mm for the probe to penetrate through such kind of aggregate. The distance stated here can be taken as a reference size of big aggregates in the remolded clayey soil, and a more reasonable interpretation may be a relatively separated area with certain average structural strength.

Sullage

The last soil sample is a cup of sullage made by completely mixing clay powder with distilled water into viscous paste, which has cured for about 48 h to attain enough plasticity and strength. Penetration results obtained by the micropenetrometer are shown in Fig. 7. It is unfortunate that the structural strength of this kind of soft soil is too low to detect by the micropenetrometer. Almost all the end resistances for this sullage are lower than 0.1 N, which is the resolution of the load cell. Thus, fluctuation in the end resistance curve is no longer representative of its microscopic structural strength, but of the deviation of the apparatus. Despite such deviations, part of the end resistance in the first 4-mm penetration is higher than 0.1 N, which still can stand for the structural strength in sullage surface. Wide exposure in the air, intensive evaporation, and then quick contraction accelerate the formation of a hard layer in sullage surface. Therefore, if penetration tests on the sample are conducted regularly, the consolidation rate from the angle of structural strength should be measured.

Flour Dough Test

Finally, as a simple but typical application in analysis of three-dimensional structural strength distribution in soft soils, a block of flour dough was prepared and tested with the micropenetrometer. After having been uniformly mixed with distilled water, the flour is kneaded into a block of dough. Before it is put into the sample container for measurement, the dough has cured in air under normal temperature for half an hour. Moisture content of the sample dough is about 40 %.

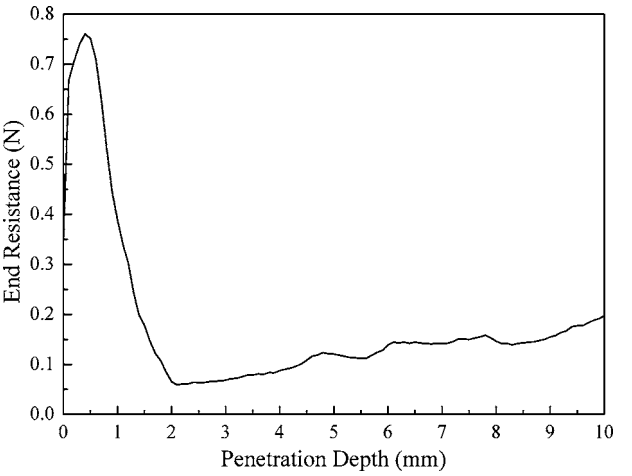

FIG. 8—*Penetration end resistance curve of the flour dough.*

Normally we will take it for granted that the flour dough will become homogeneous, i.e., the structural strength inside the dough should basically be equal everywhere, but the real thing is a little different from what we thought. Figure 8 is a typical relation curve of probe end resistance and its penetration depth. In the first 1-mm penetration depth, the end resistance is much higher than that of the rest. The maximum end resistance is between 0.7 and 0.8 N. When the penetration depth is larger than 1 mm (or 2 mm somewhere else) the resistance force basically keeps steady between 0.1 and 0.2 N, nevertheless there still exist some fluctuations, which just reflect the detailed structural strength variation inside the dough.

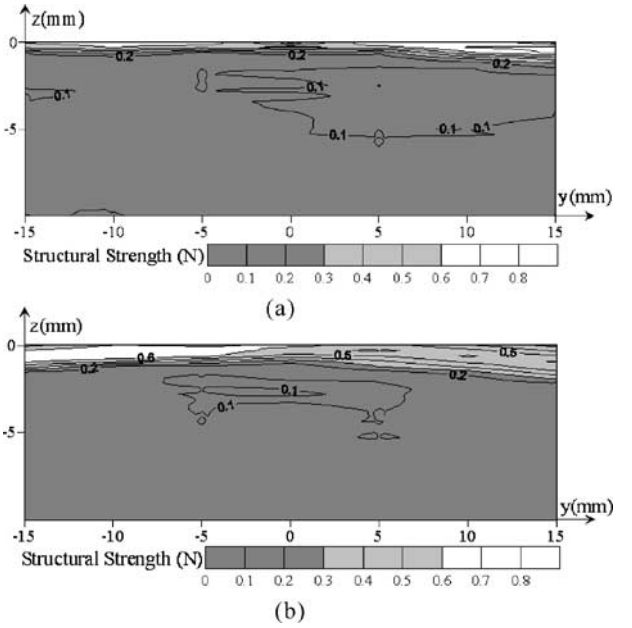

FIG. 9—*Isoline maps of structural strength distribution on two parallel vertical sections.*

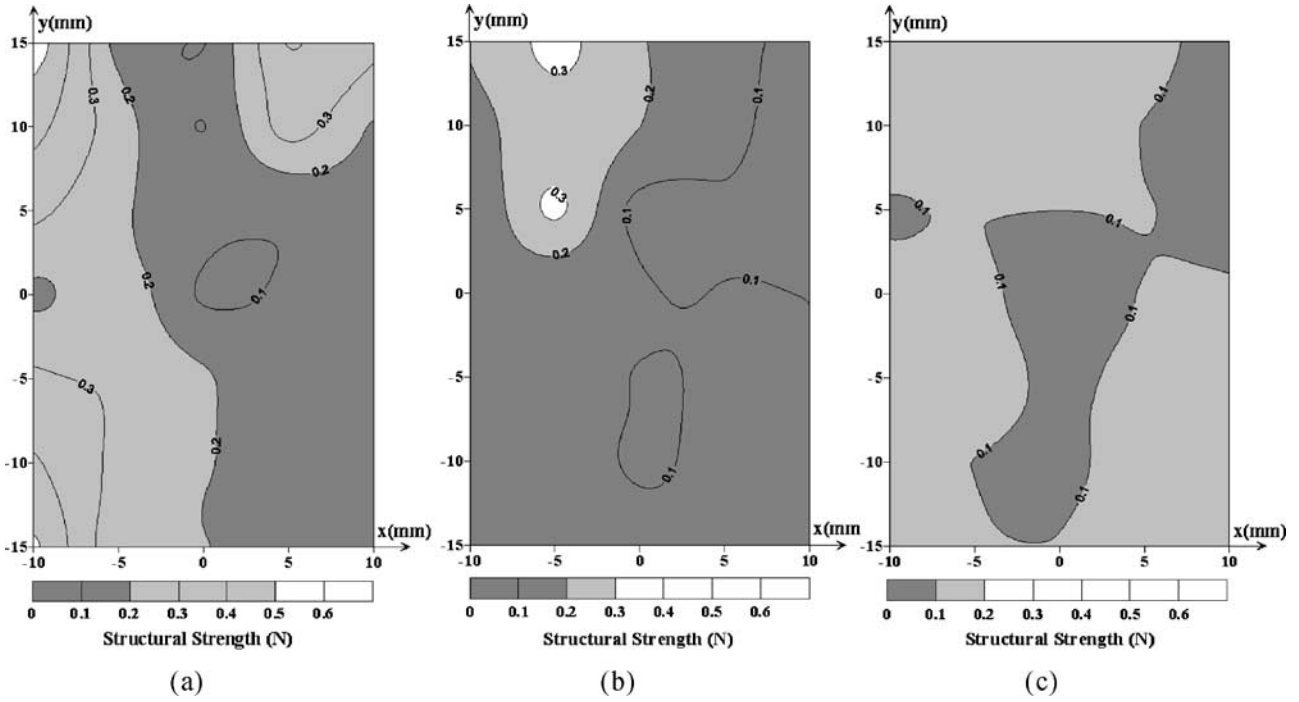

FIG. 10—*Isoline maps of structural strength distribution on three parallel transverse sections.*

According to the analysis clew above, isoline maps of the structural strength distribution on two parallel vertical sections were derived from sampled data at grid nodes through interpolation. From Fig. 9 it also can be seen that structural strength in the top layer of the dough is higher than that of the inner part, and most regions inside the dough have approximately equivalent strength value. The surface layer of dough is easy to lose moisture and become dryer and harder when exposed in air, and later a crust will be formed. However, there also exist some regions with strength value of small difference. Figure 10 are three selected strength distribution isoline maps of transverse section in the top layer of flour dough. It is obvious that there are more detailed structures inside a seemingly uniform material. For example, in the rectangular scope, whose x value is from 0 to +5 mm, and y value between 0 to +5 mm, there is a soft area.

Despite these detailed microstructures, the dough still can be looked on as a relatively homogeneous object if the maximum acceptable deviation of about 0.8 N for the structural strength is taken into consideration. This means that a new statistical quantitative standard can be established to judge that to what degree a soil can be seen as a homogeneous object from the angle of structural strength. However, establishment of the standard depends on detailed structural strength values and requirements of the practical problems being studied.

Conclusions and Discussion

Development and application tests of the micropenetrometer provide an effective analysis tool for the structural strength distribution inside soft soils, which could hardly be achieved by most traditional experimental apparatus. The paper shows that SMP-1 micropenetrometer is applicable in the structural strength analysis inside soft soils. Penetration parameters such as the probe diameter, penetration speed or sampling period can be selected according to the soil type and experimental objective. With the micropenetrometer, relation curves of probe end resistance and penetration depth, and then three-dimensional structural strength distribution along vertical or transverse sections can be obtained. The micropenetrometer also puts forward an experimental method that how to judge the isotropy or anisotropy of a soil quantitatively from the angle of structural strength in soil.

Application tests indicate that obvious difference in the penetration resistance curves of soft soils is closely related to their textural properties.

It is also found that the structural strength inside soils is sensitive to differences in soil moisture, so the micropenetrometer can be adopted to monitor the moisture infiltration and movement inside a soil. With penetration resistance and depth data of good quality, it also should be possible to use some micromechanical model to recover microstructural and micromechanical properties and use them to characterize the soil.

Acknowledgments

This work is a part of research project about fabric and strength of aggregates in unsaturated soil, which is supported by Natural Science Fund for Distinguished Young Scholars of China (No. 40225006) and National Natural Science Foundation of China (No. 40172089).

References

Ayers, P. D. and Bowen, H. D., 1987, "Predicting Soil Density Using Cone Penetration Resistance and Moisture Profile," *Transactions of American Society of Agricultural Engineers*, Vol. 30, pp. 1331–1336.

Braunack, M. V., Hewitt, J. S., and Dexter, A. R., 1979, "Brittle Fracture of Soil Aggregates and the Compaction of Aggregate Beds," *J. Soil Sci.*, Vol. 30, pp. 653–667.

Fukue, M., Minato, T., Horibe, H., and Taya, N., 1999, "The Microstructures of Clay Given by Resistivity Measurements," *Eng. Geol.* (*Amsterdam*), Vol. 54, pp. 43–53.

Gill, W. R., 1968, "Influence of Compaction Hardening on Penetration Resistance," *Transactions of American Society of Agricultural Engineers*, Vol. 11, No. 6, pp. 741–745.

Hadas, A., 1987, "Long-term Tillage Practice Effects on Soil Aggregation Models and Strength," *Soil Sci. Soc. Am. J.*, Vol. 51, pp. 191–197.

Henderson, C. W. L., 1989, "Using a Penetrometer to Predict the Effects of Soil Compaction on the Growth and Yield of Wheat on Uniform Sandy Soils," *Australian Journal of Agricultural Research*, Vol. 40, pp. 497–508.

Katti, D. R. and Shanmugasundaram, V., 2001, "Influence of Swelling on the Microstructure of Expansive Clays," *Can. Geotech. J.*, Vol. 38, pp. 175–182.

Lapierre, C., Leroueil, S., and Locat, J., 1990, "Mercury Intrusion and Permeability of Louiseville Clay," *Can. Geotech. J.*, Vol. 27, pp. 761–773.

Li, X. and Zhang, D., 1999, "Application of CT in Analysis of Structure of Compacted Soil," *Chinese Rock and Soil Mechanics*, Vol. 20, No. 2, pp. 62–66.

Liu, Z., Shi, B., and Wang, B., 2004, "Quantitative Research on Micropores of Modified Expansive Soils," *Chinese J. Geotech. Eng.*, Vol. 26, No. 4, pp. 526–530.

Otani, J., Obara, Y., and Mukunoki, T., 1997, "Characterization of Failure and Density Distribution in Soils Using X-ray CT Scanner," *Proceedings of China-Japan Joint Symposium on Recent Development of Theory and Practice in Geotechnology*, Shanghai, China, pp. 45–50.

Prapaharan, S., Altschaeffl, A. G., and Dempsey, B. J., 1985, "Moisture Curve of Compacted Clay: Mercury Intrusion Method," *J. Geotech. Eng.*, ASCE, Vol. 111, No. 9, pp. 1139–1143.

Schneebeli, M. and Johnson, J. B., 1998, "A Constant Speed Penetrometer for High-resolution Snow Stratigraphy," *Ann. Glaciol.*, Vol. 26, pp. 107–111.

Shi, B. and Li, S., 1995, "Quantitative Approach on SEM Images of Microstructure of Clay Soils," *Sci. China, Ser. B: Chem., Life Sci., Earth Sci.*, Vol. 38, No. 6, pp. 741–748.

Smart, P. and Tovey, N. K., 1966, "Optical Microscopy and Soil Structure," *Nature* (*London*), Vol. 210, pp. 1400.

Tamotsu, K., Satoru, S., Naofumi, K., Seichi, S., and Hiroshi, O., 2001, "Observation of Microstructures of Compacted Bentonite by Microfocus X-ray Computerized Tomography (Micro-CT)," *J. Nucl. Sci. Technol.*, Vol. 38, No. 8, pp. 697–699.

Tovey, N. K. and Krinsley, D. H., 1992, "Mapping of the Orientation of Fine-grained Minerals in Soils and Sediments," *Bull. Int. Assoc. Eng. Geol.*, Vol. 46, pp. 93–101.

Whiteley, G. M. and Dexter, A. R., 1981, "The Dependence of Soil Penetrometer Pressure on Penetrometer Size," *J. Agric. Eng. Res.*, Vol. 26, pp. 467–476.